The relation between protein adsorption and hemocompatibility of antifouling polymer brushes

*Zuzana Riedelová, Andres de los Santos Pereira, Jan Svoboda, Ognen Pop-Georgievski, Pavel Májek, Klára Pečánková, Filip Dyčka, Cesar Rodriguez-Emmenegger, Tomáš Riedel**

T. Riedel, A. de los Santos Pereira, Z. Riedelová, J. Svoboda, O. Pop-Georgievski
Institute of Macromolecular Chemistry, Czech Academy of Sciences, Heyrovsky sq. 2, Prague, 162 06, Czech Republic
E-mail: riedel@imc.cas.cz

P. Májek, K. Pečánková
Institute of Hematology and Blood Transfusion, U Nemocnice 1, Prague, 128 00, Czech Republic

F. Dyčka
Faculty of Science, University of South Bohemia, Branišovská 1760, 370 05 České Budějovice, Czech Republic

C. Rodriguez-Emmenegger
Institute for Bioengineering of Catalonia (IBEC), The Barcelona Institute of Science and Technology (BIST), Carrer de Baldiri Reixac, 10, 12, 08028 Barcelona, Spain

C. Rodriguez-Emmenegger
Institució Catalana de Recerca i Estudis Avançats (ICREA), Passeig Lluís Companys 23, 08010 Barcelona, Spain

C. Rodriguez-Emmenegger
DWI - Leibniz Institute for Interactive Materials, Forckenbeckstraße 50, Aachen, D-52074, Germany

Keywords: polymer brushes, antifouling surfaces, MS identification, hemocompatibility, protein adsorption

Abstract

Whenever an artificial surface comes into contact with blood, proteins are rapidly adsorbed onto its surface. This phenomenon, termed fouling, is then followed by a series of undesired reactions involving activation of complement or the coagulation cascade and adhesion of

leukocytes and platelets leading to thrombus formation. Thus, considerable efforts are directed towards the preparation of fouling-resistant surfaces with the best possible hemocompatibility. Herein, a comprehensive hemocompatibility study after heparinized blood contact with seven polymer brushes prepared by surface-initiated atom transfer radical polymerization is reported. We quantified the fouling resistance and analyzed thrombus formation and deposition of blood cellular components on the coatings, Moreover, we performed identification of the remaining fouled proteins via mass spectroscopy to elucidate their influence on the surface hemocompatibility. Compared with an unmodified glass surface, the grafting of polymer brushes minimizes the adhesion of platelets and leukocytes and prevents the thrombus formation. The fouling from undiluted blood plasma was reduced by up to 99%. Most of the identified proteins are connected with the initial events of foreign body reaction towards biomaterial (coagulation cascade proteins, complement component and inflammatory proteins). In addition, several proteins that were not previously linked with blood-biomaterial interaction are presented and discussed.

1. Introduction

Hundreds of millions of blood-contacting medical devices are used worldwide every year, and the number is constantly increasing.[1-3] Despite the considerable diversity, these devices can be divided into three categories: indwelling (e.g. intravenous cannulas), implanted (e.g. coronary stents) or extracorporeal (e.g. dialysis circuits, extracorporeal membrane oxygenators).[4,5] These three groups differ not only in their use, but also in the length of time they interface blood. The contact time can range from just few hours to even years. However, regardless of the type of device or time of use, they all share the same challenge, the exposure of blood to a surface different than native endothelium.[4] Although blood-contacting medical devices have become an integral and successful part of modern medicine, their use is not without problems originating from their exposure to blood. When any artificial material comes into contact with a biological fluid that contains soluble proteins, the proteins rapidly adsorb and form a monolayer on the surface.[6-8] This non-specific interaction between protein and surface is called fouling, which is a key problem in medical and biotechnological applications. Adsorbed proteins together with platelet adhesion can lead to complement activation.[9] At the same time, leukocytes may be attracted, allowing the immune system to identify these surfaces as a foreign body with concomitant deleterious effects. Another undesirable effect of protein adsorption is the possibility of initiating a coagulation cascade. The consequence of the above effects is a progressive deterioration of device function which can lead to thromboembolic complications causing severe or even fatal complications.[10]

A number of different synthetic and natural coatings has been developed in order to ameliorate the effect of fouling.[11,12] Typically, models of individual proteins (BSA, HSA, fibrinogen)

have been used to characterize fouling resistance of artificial surfaces [13,14]; however, as we have shown these models are not sufficient to demonstrate fouling resistance to complex biological media such as blood or blood plasma.[7,13,14] Complex biological media, especially blood, are much more challenging than models consisting of individual proteins. Usually, such oversimplify models fail to account for the synergies between adsorbing proteins.[13] The complexity of the full blood interaction can be illustrated on leukocytes and platelets. Leukocytes are involved in many processes related to inflammation or the response to infection. The leukocyte adhesion process itself may be mediated by pre-adhesion of platelets or platelet aggregates, additional particles/cells not present in simplified models of fouling resistance. In addition, platelet activation may, for example, initiate thrombosis. Another example may be red blood cells, which are not usually involved in thrombosis processes, therefore the process of direct adhesion was considered less important. However, red blood cells have been shown to mechanically influence the diffusive and convective transport of other blood elements.[15] It is therefore essential that materials coming into contact with blood are tested not on simplified models of individual proteins (HSA, fibrinogen, IgG) or cells (red blood cells, platelets, leukocytes) but directly with whole blood.

A large number of surface modifications have been developed to reduce fouling on material surfaces. Poly(ethylene glycol) (PEG) remains as the most frequently used polymer as it provides hydrophilization of the surface (reduction of interfacial energy) and steric repulsion based on its inherent flexibility. However, superior antifouling properties were mainly achieved by "grafting from" of various hydrophilic polymers including poly[(oligo(ethylene glycol) methyl ether methacrylate)] (poly(MeOEGMA)), poly(2-hydroxyethyl methacrylate) (poly(HEMA)), and poly[*N*-(2-hydroxypropyl) methacrylamide] (poly(HPMA)) or electroneutral zwitterionic polymers such as poly(carboxybetaine acrylamide) and methacrylamide (poly(CBAA), poly(CBMAA)), poly(sulfobetaine methacrylamide) (poly(SBMA)), and poly(phosphorylcholine methacrylamide) (poly(PCMA)) using surface-initiated polymerizations.[16,17] These polymer modifications totally suppress fouling from individual protein solutions and often reach over 90% reduction of protein adsorption from undiluted blood plasma. Poly(HPMA), poly(CBAA), poly(CBMAA) and a copolymer poly(HPMA-co-CBMAA) reach ultralow fouling below 3 $ng \cdot cm^{-2}$, which was not achieved by any other surface modification.[8,18,19] These surface chemistries served as the basis for the development of more advanced coatings that while displaying brush-like interfaces were readily applicable to almost any material's surface.[20-22] Moreover, they could be combined with bioactive molecules to even eliminate thrombii formed.[23,24]

The prevention of fouling from blood plasma has been postulated as a proxy to predict whether a coating improves the hemocompatibility,[25] however, the nature and types of proteins involved in fouling from whole blood remains unknown. In this study, we analyzed the

hemocompatibility of seven different polymers – poly(HEMA), poly(HPMA), poly(MeOEGMA), poly(SBMA), poly(PCMA), poly(CBAA), and poly(HPMA-co-CBMAA). To gain insight into the factors affecting hemocompatibility, we contacted the surfaces with freshly drawn blood to observe cellular attachment, measured protein adsorption from plasma, and performed mass-spectrometric identification of the adsorbed proteins. The results revealed the interplay between surface physicochemical properties, identity and amount of adsorbed proteins, and attachment and activation of various blood cells.

2. Results and discussion

2.1. Synthesis of polymer brushes

All brushes assessed in this studied were grafted from a monolayer of initiator on glass using atom transfer radical polymerization (ATRP). Based on previously reported fouling resistance, a set of six homopolymer and one copolymer brushes was selected (**Scheme 1**). The corresponding monomers were polymerized using SI-ATRP from the initiator SAM using protocols previously reported for each monomer.[14,26-29] The polymerization conditions and time were tuned to target a thickness between 20 and 30 nm in the dry state (**Supporting Information, Table S1**). The thickness was controlled by thickness measurements via ellipsometry on Si wafer chips coated in parallel with the same SAM and polymer brushes.

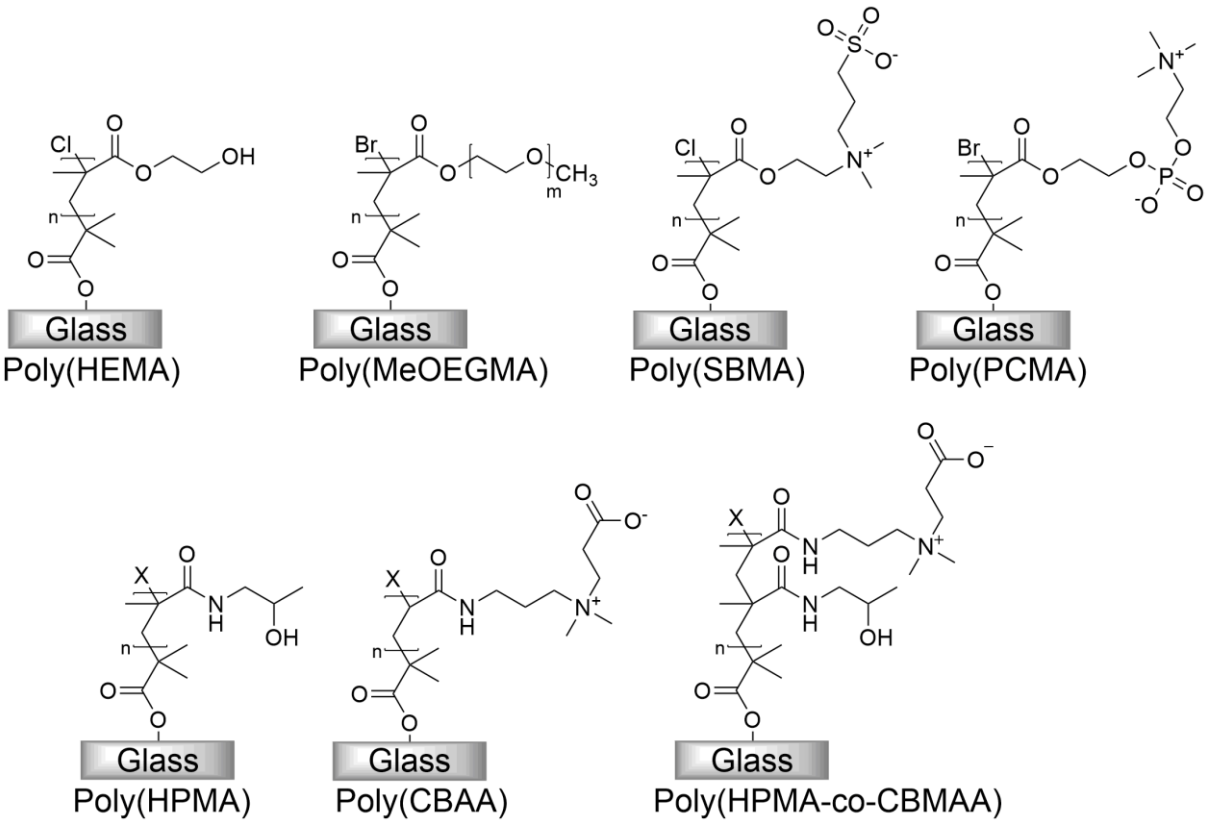

Scheme 1. Chemical structures of the polymer brushes employed.

2.2. Chemical characterization

X-ray photoelectron spectroscopy (XPS) was utilized to probe the chemical composition of the synthesized polymer brushes. Deconvolution of the acquired high-resolution spectra of the C1s region corresponds to the expected chemical structures of the polymer brushes (**Figure 1**). The C–C, C–H contribution at 285.0 eV is marked in the spectra of all brushes. The spectra of poly(HEMA), poly(MeOEGMA), poly(SBMA) and poly(PCMA) present a contribution at 289.0 eV, which arises from the ester carbon of the methacrylate group. Poly(HPMA), poly(CBAA), and poly(HPMA-co-CBMAA) display a component at 288.0 eV, corresponding to the (meth)acrylamide carbon. Additionally, poly(CBAA) shows a contribution at 288 eV coming from the COO– group. The contribution from the alpha carbon to the ester/amide shows a secondary shift, appearing at 285.4 eV. For poly(MeOEGMA) the signal at 286.6 eV dominates due to the abundance of C–O in the side chain. The C–O component is also marked in the C1s spectrum of poly(HEMA) and appears for all polymers except poly(CBAA). In the spectrum of the zwitterionic brushes poly(SBMA), poly(PCMA), and poly(CBAA) the strong contribution at 286.4 eV has its origin in the $C–N^+$ carbons. For the copolymer poly(HPMA-co-CBMAA) this $C–N^+$ component appears together with the C–N, increasing its intensity. Importantly, the N1s spectra of the nitrogen-containing polymers show signals corresponding to their expected compositions and poly(SBMA) and poly(PCMA) show the presence of the predicted species in the S2p and P2p spectra, respectively (**Supporting Information, Figure S1**).

Further confirmation of the success of the formation of the polymer brush coatings is given by the dynamic water contact angles (CA, Supporting information, Table S1). Zwitterionic brushes in particular display very high wettability, with receding CA below 10º, due to the strong water interaction of the zwitterionic dipoles. Poly(HEMA), poly(MeOEGMA), and poly(HPMA) show marked CA hysteresis, which can be explained by the reorientation of the polymer hydrophilic groups.[30] Due to their hydrophilicity, these polymer brushes swell in water. Previous studies of similar brushes indicate that their swelling ratios are comparable.[19,31-33]

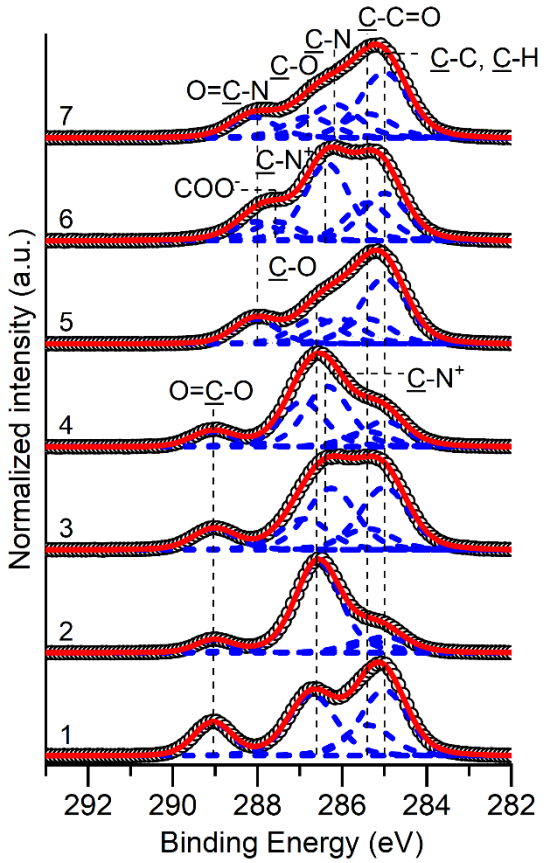

Figure 1. High-resolution XPS spectra of the C1s region of: (1) poly(HEMA); (2) poly(MeOEGMA); (3) poly(SBMA); (4) poly(PCMA); (5) poly(HPMA); (6) poly(CBAA); and (7) poly(HPMA-co-CBMAA) brushes.

2.3. Fouling from blood plasma

Pooled citrated blood plasma was contacted with the polymer brushes for 30 minutes and the amount of adsorbed protein was analyzed using XPS. Differential N1s XPS spectra were obtained from polymer brushes before and after being contacted with blood plasma. The reduction of fouling was approximated by comparing the area under the obtained differential N1s spectrum for each polymer brush with the area under the N1s spectrum obtained from plasma deposit on glass (**Supporting Information, Figure S2**). All the polymer coatings significantly reduced the fouling compared to glass. Poly(HEMA) and poly(MeOEGMA) achieved 79% and 93% fouling reduction, respectively. The zwitterionic polymers showed fouling reduction of 57% for poly(PCMA), 82% for poly(SBMA) and 95% for poly(CBAA). Poly(HPMA) and its copolymer poly(HPMA-co-CBMAA) displayed fouling reduction 99% and 96%, respectively. The obtained results are in agreement with previously published data of blood plasma fouling measured by surface plasmon resonance on gold surfaces coated with the same brushes. This indicates that the polymer brush coating on glass and gold surface have similar properties. Zwitterionic polymers have typically shown excellent resistance to single protein solutions.[34] However, both poly(PCMA) and poly(SBMA) suffered from a high extent

of protein fouling when contacted with blood plasma.[14] On the other hand, poly(CBAA) reached very low fouling from blood plasma. This extraordinary resistance of poly(CBAA) was previously attributed to high wettability, electrostatically induced hydration, and to its kosmotropic effect.[11] In our previous studies, we have shown that poly(HPMA), despite having moderate wettability (Supporting Information, Table S1) and being a hydrogen bond donor, can suppress the blood plasma fouling to a level comparable to the best zwitterionic polymers.[8]

2.4. Hemocompatibility

The polymer brushes were exposed to heparinized blood in a dynamic model, which simulated the contact of blood with a graft implanted into a patient's cardiovascular system. Blood is usually anticoagulated with heparin during several types of surgery, for example those involving cardiopulmonary bypass, or hemodialysis. The adhesion of the main cellular component (RBCs, platelets and leukocytes) to the surface and the activation of the coagulation cascade (via fibrin/thrombus formation) was analyzed. In addition, we also focused on the plasma marker of complement activation SC5b-9 after blood contact with the sample.

Figure 2 shows deposit on the tested samples after exposure to heparinized blood under dynamic conditions. The adhesion of the blood components (red blood cells, leukocytes, and platelets) after 1h incubation was evaluated using SEM. In glass we observed total coverage of the surface by a three-dimensional clot. The clot entraps a large number of leukocytes, platelets and red blood cells, being the latter those of higher count. The application of a polymer brush coating strongly suppressed cell adhesion. Only few spread leukocytes and adhered platelets, if any, adhered on the coatings.

Leukocytes and platelet adhesion are a critical step for biomaterials contacting blood. Their adhesion determines the subsequent fate of the material. While platelet adhesion leads to platelet activation and aggregation, which is followed by the initiation of the coagulation cascade and thrombus formation, the leukocytes trigger an inflammatory response of the organism to the presence of a foreign material leading to a foreign body reaction. The foreign body reaction is an unavoidable process which takes place whenever any material becomes implanted into the body. On the other hand, the presence of RBCs in the deposits on the tested samples has no informative value, as the main biological function of RBC is oxygen transport and their presence in the deposits is mainly due to entrapment (*e.g.* by fibrin in thrombus) or by improper washing procedure.

We quantified the surface coverage with adherent RBCs, leukocytes, and platelets from high-magnification SEM images, which allowed identifying the type of adherent cells based on size

and morphology. The adherent leukocytes varied from 0 to 0.34% surface coverage (**Figure 3A**). No leukocytes were observed on poly(HEMA), poly(MeOEGMA), and poly(PCMA). The highest number of leukocytes was present in the deposit on poly(HPMA-co-CBMAA), 0.34±0.48%. Importantly, a very low number of adherent leukocytes was observed on the antifouling surfaces, in agreement with our previous work dealing with adsorption of isolated leukocytes and from citrated blood. The adhesion of leukocytes has been previously linked with the fibrinogen adsorption; therefore, preventing the protein fouling might be one parameter explaining the decreased leukocyte adhesion on the polymer brushes.[35]

Platelets usually adhere very fast on any material other than healthy endothelium and after adhesion they become activated and tend to aggregate. This phenomenon was visible on the bare glass surface. The platelets attached on glass supported the activation of coagulation cascade and as a result thrombus was formed on the surface containing entrapped RBC, platelets and leukocytes. In contrast, only very few individual platelets and their aggregates could be observed on the polymer brushes without formation of the thrombus. The surface coverage of adherent platelets was in the range of 0.01 to 8.8%. Poly(HEMA) had the highest number of adherent platelets 8.8±2.1%, while the other polymer brushes had less than 0.02% attached platelets on their surface.

Regarding the RBC adhesion, only a few RBCs were visible on all polymer brushes in the range from 0 to 0.18%. The presence of RBC is not related to the initiation of thrombosis nor inflammation; therefore, the process of RBC attachment is considered to be an artefact of minor importance.

The plasma marker of complement activation, SC5b-9, was evaluated after 1h contact of heparinized blood (**Figure 3B**). A high level of complement activation was observed on poly(HPMA-co-CBMAA) and on poly(HPMA). This suggests that the poly(HPMA) could be a strong complement activator. Another hydroxyl group bearing polymer poly(HEMA) did not activate the complement to such an extent as the copolymer. Nevertheless, the complement activation on poly(HEMA) was significant compared to control. It should be noted, that poly(HEMA) was previously reported to activate the complement through the “tick-over” mechanism of spontaneous C3 activation, but this effect was strongly dependent on the donor.[26] In other words, poly(HEMA) can strongly activate complement when contacted with blood from certain donors but much less strongly on blood from other donors. The remaining polymers did not significantly activate the complement. Surprisingly, bare glass displayed low complement activation in spite of adsorbing a large number of proteins and cells. We hypothesize that the rapid adsorption of these components conceals the silanol groups thereby precluding the complement activation.

In general, the test shows an excellent hemocompatibility of all tested polymer brushes (poly(HEMA); poly(HPMA); poly(HPMA-co-CBMAA); poly(SBMA); poly(CBAA); poly(MeOEGMA); and poly(PCMA) compared to unmodified glass substrate. The very good hemocompatibility of the polymer brushes prepared on glass from a silane initiator can be attributed to the antifouling properties of the individual polymers. However, the structure of the polymer, e.g. the presence, availability, and reactivity of the –OH groups, can significantly influence the performance in full blood as shown in the case of poly(HPMA), poly(HEMA) and poly(HPMA-co-CBMAA).

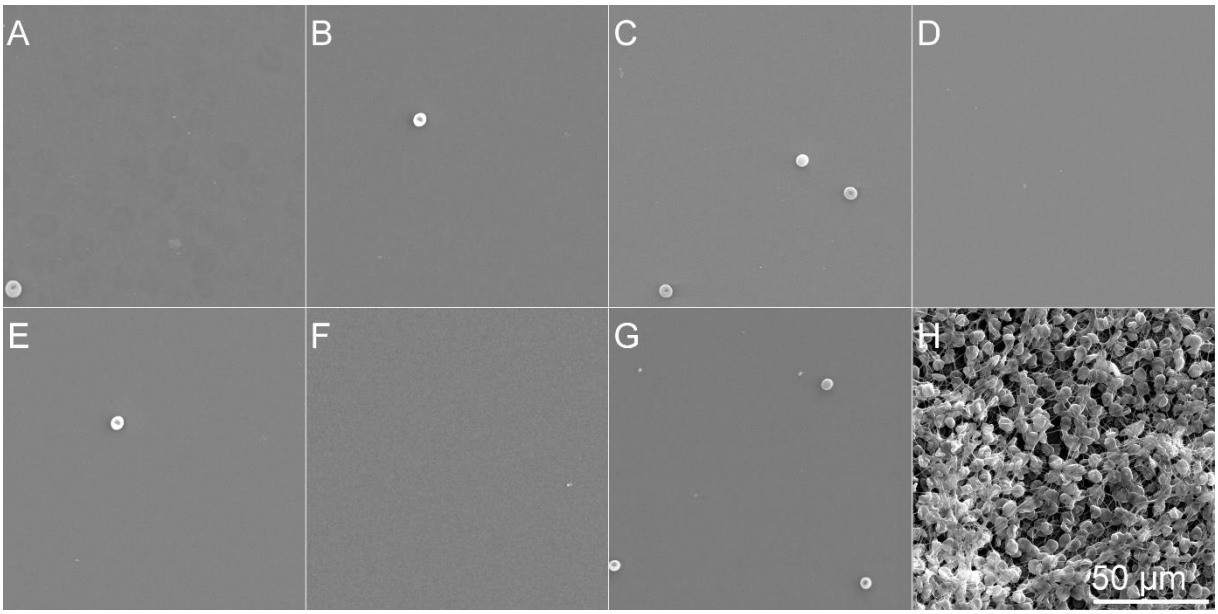

Figure 2. A scanning electron micrograph of polymer coatings on glass exposed to heparinized human blood: A) poly(HEMA); B) poly(MeOEGMA); C) poly(SBMA); D) poly(PCMA); E) poly(HPMA); F) poly(CBAA); G) poly(HPMA-co-CBMAA); H) reference glass substrate.

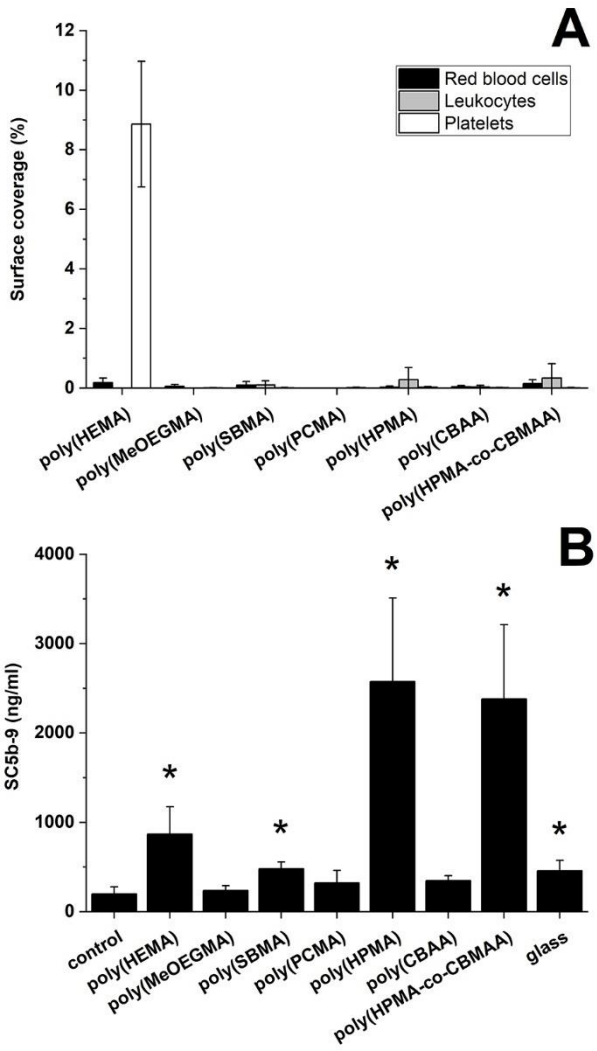

Figure 3. A) The amount of adherent blood components on polymer brushes on glass after 1h contact with heparinized blood. RBC – red blood cells, WBC – white blood cells, PLT – platelets. B) Complement marker of activation SC5b-9 analyzed after heparinized blood contact. The data are given as mean with standard deviation (n = 3). * shows statistical significance compared to control ($p < 0.05$).

2.5. Identification of protein composition in fouling deposits via mass spectroscopy

The interaction of leukocytes and platelets with a surface is known to be mediated by proteins that previously deposited on the surface. While the antifouling character of the polymer brushes conferred them enhanced hemocompatibility, it does not explain it completely, as in the case of poly(PCMA). Therefore, we focused on the identification of the fouled proteins by mass spectroscopy and compared the differences among individual coatings. The surfaces were contacted with blood plasma and the deposit was removed by direct trypsinization. This approach was previously shown as an excellent model, limiting the number of necessary steps required to process the sample prior the MS identification.[13] Mass spectrometric analysis of the composition of protein deposits on the surface of polymers is based on the cleavage of proteins contained in the deposits by a suitable protease (*e.g.* bovine trypsin), separation of

these peptides by liquid chromatography and subsequent measurement of mass spectrometric spectra of the peptides. Identification of peptides/proteins is then performed by comparing the spectra of individual peptides with known spectra in a selected database. Mass spectrometry provides qualitative information about the detailed composition of proteins in a given protein deposit and quantitative information for relative comparison of the abundance of individual proteins in the deposits of each studied surface. For better understanding of the proteins involved in the fouling, we grouped the proteins according to their primary function - coagulation, complement components, immune response, lipid metabolism, acute phase proteins, transport proteins, others). The list of top 30 fouled proteins ordered by intensity is shown in the **Table 1** and heatmaps of proteins ordered according to their function are presented in **Figure 4**. The most common proteins that were identified include – Albumin, fibrinogen, IgG, complement C3, various apolipoproteins, haptoglobin, kininogen, histidine-rich glycoprotein, alpha-2-macroglobulin, kallikrein, coagulation factor XI, *etc*. Most of these proteins are connected with the initial events of foreign body reaction towards biomaterial. An expanded heatmap showing the top 100 identified proteins can be found in the SI.

Table 1. List of 30 most abundant blood plasma proteins identified in the blood plasma deposit listed in order of abundance on individual substrates (by intensity).

poly(HEMA)	poly(MeOEGMA)	poly(SBMA)	poly(PCMA)	poly(HPMA)	poly(CBAA)	poly(HPMA-co-CBMAA)	glass
Serum albumin	Serum albumin	Serum albumin	Apolipoprotein B-100	Serum albumin	Serum albumin	Serum albumin	Kininogen-1
Apolipoprotein A-I	Apolipoprotein A-I	Apolipoprotein A-I	Serum albumin	Apolipoprotein A-I	Apolipoprotein A-I	Ig mu chain C region	Histidine-rich glycoprotein
Ig mu chain C region	Ig mu chain C region	Fibrinogen alpha chain	Ig mu chain C region	Fibrinogen alpha chain	Fibrinogen alpha chain	Apolipoprotein A-I	Serum albumin
Fibrinogen alpha chain	Haptoglobin	Fibrinogen beta chain	Apolipoprotein(a)	Haptoglobin	Ig mu chain C region	Fibrinogen alpha chain	Apolipoprotein A-I
Haptoglobin	Alpha-2-macroglobulin	Fibrinogen gamma chain	Apolipoprotein A-I	Fibrinogen beta chain	Fibrinogen beta chain	Fibrinogen beta chain	Fibrinogen alpha chain
Fibrinogen beta chain	Complement C3	Haptoglobin	Fibrinogen alpha chain	Apolipoprotein B-100	Fibrinogen gamma chain	Fibrinogen gamma chain	Coagulation factor XI
Complement C3	Fibrinogen alpha chain	Complement C3	Fibrinogen beta chain	Complement C3	Complement C3	Haptoglobin	Fibrinogen beta chain
Fibrinogen gamma chain	Fibrinogen beta chain	Ig mu chain C region	Fibrinogen gamma chain	Fibrinogen gamma chain	Haptoglobin	Desmoplakin	Fibrinogen gamma chain
Alpha-2-macroglobulin	Fibrinogen gamma chain	Alpha-2-macroglobulin	Complement C3	Alpha-2-macroglobulin	Alpha-2-macroglobulin	Apolipoprotein C-I	Apolipoprotein E
Apolipoprotein B-100	Ig gamma-2 chain C region	Apolipoprotein B-100	Haptoglobin	Ig mu chain C region	Apolipoprotein B-100	Apolipoprotein E	Apolipoprotein B-100
Apolipoprotein E	Apolipoprotein A-II	Hemopexin	Alpha-2-macroglobulin	Ig gamma-2 chain C region	Apolipoprotein A-II	Dermcidin	Vitronectin
Apolipoprotein A-II	Ceruloplasmin	Ig gamma-2 chain C region	Apolipoprotein E	Apolipoprotein A-II	Apolipoprotein C-III	Alpha-2-macroglobulin	Complement C3
Ig gamma-2 chain C region	Hemopexin	Apolipoprotein A-II	Immunoglobulin J chain	Ceruloplasmin	Serotransferrin	Desmoglein-1	Apolipoprotein C-III
Hemopexin	Apolipoprotein B-100	Ceruloplasmin	Apolipoprotein C-III	Fibronectin	Apolipoprotein E	Complement C3	Apolipoprotein C-I
Ceruloplasmin	Dermcidin	Fibronectin	Apolipoprotein A-II	Hemopexin	Hemopexin	Immunoglobulin J chain	Ig mu chain C region
Alpha-1-acid glycoprotein	Alpha-1-acid glycoprotein	Alpha-1-acid glycoprotein	Ig gamma-2 chain C region	Inter-alpha-trypsin inhibitor heavy chain	Ig gamma-2 chain C region	Caspase-14	Clusterin
Clusterin	Immunoglobulin J chain	Vitronectin	Hemopexin	Inter-alpha-trypsin inhibitor heavy chain	Ceruloplasmin	Desmocollin-1	Haptoglobin
Apolipoprotein C-III	Fibronectin	Apolipoprotein C-III	Ceruloplasmin	Apolipoprotein E	Fibronectin	Junction plakoglobin	Inter-alpha-trypsin inhibitor heavy chain
Fibronectin	Inter-alpha-trypsin inhibitor heavy chain	Apolipoprotein A-IV	Apolipoprotein C-I	Alpha-1-acid glycoprotein	Actin	Apolipoprotein C-III	Angiogenin
Inter-alpha-trypsin inhibitor heavy chain	Apolipoprotein E	Inter-alpha-trypsin inhibitor heavy chain	Fibronectin	Inter-alpha-trypsin inhibitor heavy chain	Alpha-1-antitrypsin	Ig gamma-2 chain C region	Apolipoprotein A-II
Apolipoprotein A-IV	Apolipoprotein C-III	Inter-alpha-trypsin inhibitor heavy chain	Clusterin	Apolipoprotein C-III	Clusterin	Serotransferrin	Apolipoprotein A-IV
Immunoglobulin J chain	Complement factor B	Kininogen-1	CD5 antigen-like	Vitronectin	Apolipoprotein C-I	Apolipoprotein A-II	Alpha-2-macroglobulin
Kininogen-1	Alpha-1B-glycoprotein	Alpha-2-HS-glycoprotein	Alpha-1-antitrypsin	Complement factor H	Alpha-1-acid glycoprotein	Clusterin	Inter-alpha-trypsin inhibitor heavy chain
Serotransferrin	Kininogen-1	Clusterin	Serotransferrin	Complement factor B	Inter-alpha-trypsin inhibitor heavy chain	Calmodulin-like protein 5	Plasminogen
Apolipoprotein C-I	Serotransferrin	Complement factor B	Alpha-1-acid glycoprotein	Apolipoprotein A-IV	Apolipoprotein A-IV	Alpha-1-antitrypsin	Fibronectin
Alpha-1-antitrypsin	Inter-alpha-trypsin inhibitor heavy chain	Apolipoprotein E	Inter-alpha-trypsin inhibitor heavy chain	Alpha-2-HS-glycoprotein	Immunoglobulin J chain	Kininogen-1	Plasma kallikrein
Complement factor B	Desmoplakin	Complement factor H	Kininogen-1	Apolipoprotein C-I	Kininogen-1	Cystatin-A	Selenoprotein P
C4b-binding protein alpha chain	Apolipoprotein C-I	Apolipoprotein C-I	Vitronectin	Kininogen-1	Alpha-2-HS-glycoprotein	Luc7-like protein 3	Ig gamma-2 chain C region
Complement factor H	Clusterin	Serotransferrin	Alpha-2-HS-glycoprotein	Clusterin	Vitronectin	Gamma-glutamyltransferase E	Hemopexin
Inter-alpha-trypsin inhibitor heavy chain	Hemoglobin subunit beta	Vitamin D-binding protein	Apolipoprotein L1	Hemoglobin subunit beta	Inter-alpha-trypsin inhibitor heavy chain	Corneodesmosin	Inter-alpha-trypsin inhibitor heavy chain

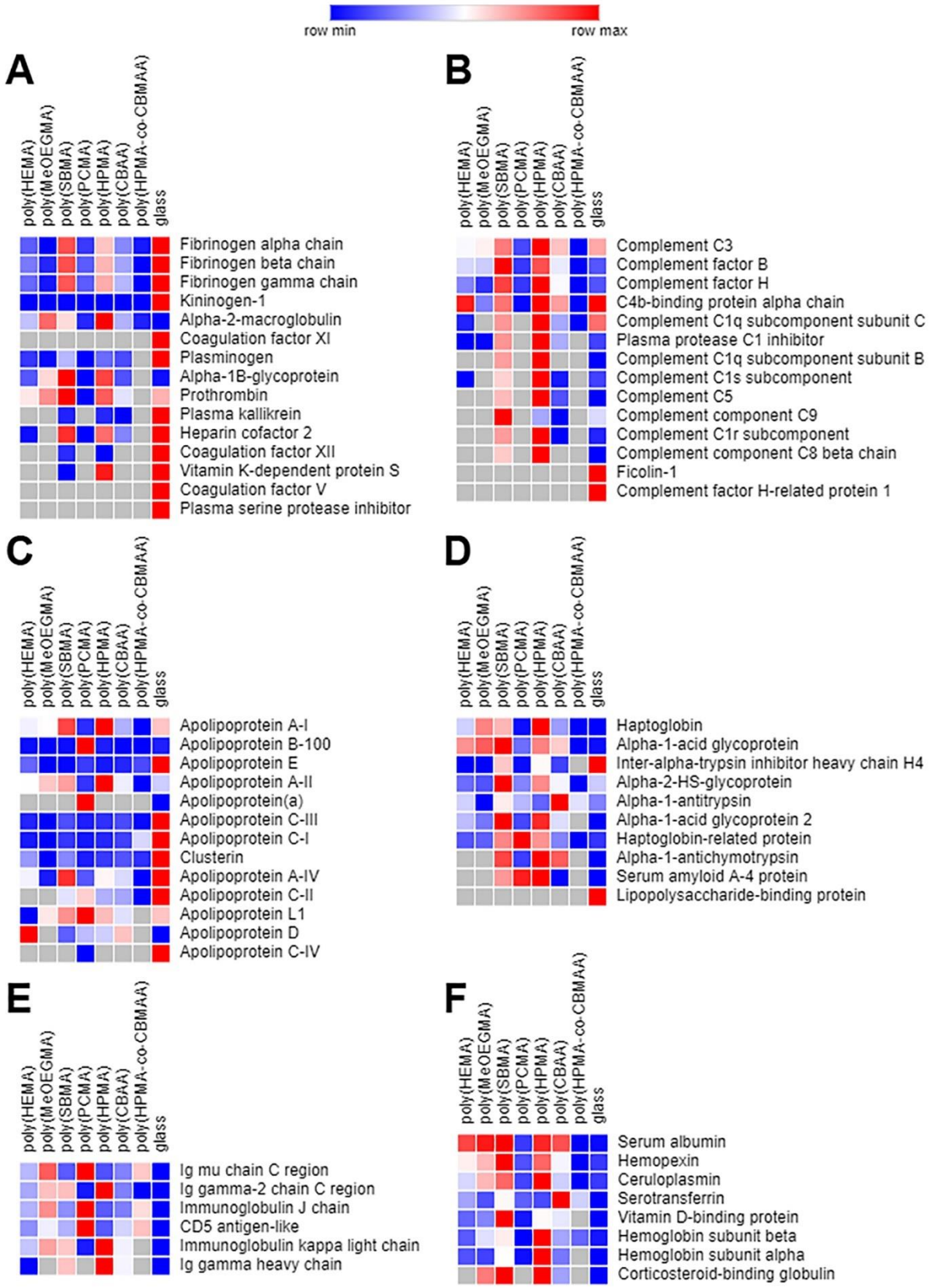

Figure 4. Heatmap of identified proteins ordered according to their function: A) coagulation; B) complement; C) lipid metabolism; D) acute phase proteins; E) immune response; F)

transport proteins. Color key indicates signal intensity of individual protein: dark blue: lowest; dark red: highest.

The most striking differences were found for the proteins taking part in coagulation (Figure 4A). In agreement with the data from hemocompatibility study, the glass surface adsorbed the highest number of proteins taking part in the coagulation cascade followed by poly(SBMA) and poly(HPMA). Glass is a well-known activator of the contact pathway of the coagulation.[36] The pathway involves high-molecular weight kininogen, prekallikrein and FXII, that becomes activated to FXIIa. FXIIa then activates its substrate FXI to FXIa.[37] All mentioned proteins were identified in high amount on the glass surface, confirming their key role in the contact pathway. Kininogen was identified in very high amount on glass, all the polymer brushes showed a hundredfold lower intensity for this protein. Plasma kallikrein was identified on glass and a negligible amount also on poly(SBMA), poly(HPMA) and poly(CBAA). As for FXII, the central protein of the contact pathway, it was identified only on glass and very small amount was identified on poly(SBMA) and poly(HPMA). Remarkably, FXI, which becomes activated by FXIIa, was identified only on the glass surface. FXI was the fifth most abundant protein in the deposit on glass. The obtained results clearly demonstrate that the polymer coating provide efficient prevention from the activation of the contact pathway of coagulation cascade.

The blood contact with any foreign material leads inevitably to complement activation, which is mainly mediated by the adsorbed plasma proteins.[38,39] The complement activation may proceed via the classical (through antibodies and C1), alternative (by a spontaneous activation of C3), or lectin (via polysaccharide structure) pathways.[40] Reducing or even preventing proteins from adsorption by an antifouling polymer coating is expected to decrease the levels of complement activation. However, as can be seen in the Figure 4, poly(HPMA) and poly(SBMA) attracted several complement proteins in higher amounts compared to other tested surfaces. C3 as well as C1 complement component proteins were identified on the surface suggesting possible activation of complement via both classical and alternative pathways. Surprisingly, very small amount of C3 and C1 were identified on the poly(HPMA-co-CBMAA) brush that contained 85% of poly(HPMA). This effect can be most probably attributed to the poly(CBMAA) that alone contained very low amounts of complement proteins adsorbed from the blood plasma. Nevertheless, the low abundance of complement components on the poly(HPMA-co-CBMAA) deposited from blood plasma is in disagreement with the SC5b-9 values measured after full blood plasma contact. It brings to attention the need to include the

effect of biological variability between individual donors.[41] We have recently presented very large differences in fouling from blood plasma among different donors on poly(HEMA) brushes reflecting different characteristic responses of the individual plasma samples.[26] **Figure 4B** shows the identified proteins belonging to the group of complement components. A very small amount of complement proteins was identified on poly(PCMA). In general, the zwitterionic poly(PCMA) brush provided the best hemocompatibility results by preventing the leukocyte, RBC, and platelet adhesion as well as by preventing the activation of complement (SC5b-9). The fact that single protein models for characterizing surface fouling resistance are not appropriate has been repeatedly demonstrated. Examples include poly(PCMA) brushes, which are able to effectively resist adsorption of individual proteins but exhibit significant fouling when exposed to blood plasma. In the context of significant fouling from complex media, it is surprising then that poly(PCMA) brush surfaces exhibit excellent hemocompatibility. Notably, while the total amount of adsorbed protein on poly(PCMA) is high, the composition of the deposit is dramatically different than on glass, namely apolipoproteins as discussed below. These results suggest that proteins (in their identity or conformation) adsorbed onto poly(PCMA) brushes do not trigger blood coagulation or mediate platelet or leukocyte adhesion. Special attention should be given to the conformation of the fouled proteins, which influences the fate of the biomaterial.[42] The importance of protein conformation is shown by the example of fibrinogen that after adsorption changes its conformation and is a critical determinant of the following platelet adhesion.[43] Because the initiation of coagulation is mediated by surface-induced activation of zymogens of certain proteins (complement components, fibrinogen, FXII, kininogen, kallikrein), it is reasonable to assume that their absence or reduction will greatly increase the potential for hemocompatibility. Indeed, in our previous work, by identifying proteins in the fouling deposits of some surfaces with increased hemocompatibility, we showed that fibrinogen was not adsorbed to any of them.[44] Similarly, FXII, kallikrein and kininogen were shown to be absent among the adsorbed proteins in poly(MeOEGMA).[13] Preventing protein adsorption is therefore an important goal for improving the hemocompatibility of materials. The difference in fouling and subsequent hemocompatibility can be illustrated by the example of zwitterionic polymer brushes and poly(HEMA). Zwitterionic polymer brushes of poly(PCMA), with their ability to mimic phosphatidylcholine in the cell membranes, exhibit lower protein adsorption than poly(HEMA), for which reduced hemocompatibility is observed.[45] The antifouling ability of the polymer brushes studied provides the coatings with excellent hemocompatibility. Nevertheless, our

results confirm that the central aspect is not the overall reduction in plasma fouling, but rather the suppression of adsorption of critical proteins, namely those involved in triggering the contact pathway of the coagulation cascade and complement system, as well as the signalling for platelet and leukocyte adhesion.

Proteins of lipid metabolism were repeatedly identified in the deposits on various biomaterials after blood and blood plasma contact.[46-48] For example, apolipoprotein A-I was identified as a main component of the protein deposits on biomaterials after blood plasma contact. We identified apolipoprotein A-I in all samples with the highest amounts on poly(SBMA) and poly(HPMA). Actually, a rather small amount of apolipoprotein A-I was identified on poly(HEMA) compared to Cornelius et al.[49] While the glass surface was fouled especially by apolipoprotein A-IV, E, C-I, C-II, C-III, and C-IV, significantly less of these proteins was present in the blood plasma deposit on the polymer brushes. It should be noted that e.g. apolipoprotein B-100, apolipoprotein (a) and apolipoprotein L1 were specific to poly(PCMA). Apolipoprotein A-II was mainly found in deposits on poly(HPMA), and apolipoprotein D was specific for poly(HEMA). The reason for such variability in the content of individual apolipoproteins remains unclear. Apolipoproteins C-I, C-II, C-III and E were recently associated with coagulation markers and thromboembolism risk.[50] On the other hand, apolipoprotein A-I as part of HDL particles has cardioprotective properties by modulation of platelet and coagulation response.[51] Apolipoprotein E has been linked with complement activation by binding through C1q and apolipoprotein B-100 can trigger C3b deposition.[52] Nevertheless, previous work by Huck[53] and us[26] did not find adsorption of apolipoprotein B-100 to be a trigger of complement activation on the surface. Poly(HPMA) and poly(SBMA) brushes showed increased complement activation that could be partially mediated by the interplay between apolipoprotein E and complement component C1q, as the blood plasma deposit on both poly(HPMA) and poly(SBMA) contained apolipoprotein E and a significantly higher level of complement component C1q compared with the other polymer brushes. Lipid metabolism has so far been studied only very generally with few exceptions. A deeper knowledge of the apolipoproteins' interaction with artificial materials could lead to development of biomaterials with improved hemocompatibility.

Furthermore, the composition of the protein deposits from plasma on bare glass and the polymer brushes differed in several other ways. For example, histidine-rich glycoprotein was found mainly on glass and very small amount was identified on all polymers brushes. Histidine-rich glycoprotein modulates the immune, vascular and coagulation systems by interaction with

several complement proteins and proteins of coagulation cascade.[54,55] It inhibits contact-initiated coagulation by binding to activated FXIIa [56,57], and it has been shown that precoating nanoparticles with histidine-rich glycoprotein decreases their uptake due to its dysopsonin activity.[58] Vitronectin and angiogenin were identified mainly on the glass while very little vitronectin or no angiogenin was identified on polymer brushes. Vitronectin is a multifunctional adhesive glycoprotein providing regulatory link between cell adhesion, humoral defense mechanisms, and cell invasion[59] while angiogenin induces angiogenesis by activating vessel endothelial and smooth muscle cells.[60] Other interesting proteins identified in significantly higher amount on polymer brushes compared to glass surface were alpha-1-acid glycoprotein, alpha-2-macroglobulin, alpha-1B-glycoprotein and haptoglobin. Alpha-1-acid glycoprotein is an acute-phase protein and several studies have indicated that it is involved in modulating inflammatory and immune responses.[61] A recent study showed higher quantities of alpha-1-acid glycoprotein on PEG hydrogels and suggested that it may be involved in mediating polymorphonuclear leukocytes primary granule release.[62] Alpha-2-macroglobulin, alpha-1B-glycoprotein and haptoglobin were not previously linked with protein deposit on biomaterial after blood contact. The presence of these proteins and their role in the blood plasma contact requires further investigations. Moreover, further work should analyze the protein adsorption kinetics and aim to elucidate the change in composition of the protein deposits over time, as it may reflect the presence of active processes.

3. Conclusion

We report a comprehensive hemocompatibility study after heparinized blood contact with seven polymer brushes prepared by surface-initiated atom transfer radical polymerization. The polymers were thoroughly characterized by XPS, dynamic water contact angle and spectroscopic ellipsometry. Reduction of protein fouling was analyzed and compared to the unmodified glass surface. In addition, the fouled proteins were identified by mass spectrometry. The polymer brushes reduced the fouling from undiluted blood plasma by up to 99%. In general, the grafting of polymer brushes minimized the adhesion of platelets and leukocytes and prevented thrombus formation. Fouling prevention from blood plasma is an effective avenue to improve hemocompatibility. Nevertheless, the contact with full blood is very complex due to high variability not only in amount but also in composition of the protein deposits and potential conformational changes and activation of enzymatic activity. In this regard, protein identification is shown to be a key element in understanding these interactions towards the

design of hemocompatible artificial surfaces. An example is the glass surface that adsorbed the largest amount of proteins involved in the coagulation cascade. These proteins were significantly reduced or eliminated from fouling on other polymer coatings, resulting in effective prevention from contact pathway activation.

Nevertheless, it was shown that mere information on the total amount of proteins in the deposit does not predict hemocompatibility. This was illustrated by the example of a poly(PCMA) brush that showed significant fouling on contact with blood plasma, but at the same time excellent hemocompatibility. In this regard, special attention should be given to the identity and conformation of the fouled proteins that influence the fate of the biomaterial. Further work should aim to elucidate the changes in conformation and activity of the identified proteins on polymer brushes, for example using circular dichroism. This report provides an in-depth analysis of the proteins interacting with various hydrophilic and electroneutral antifouling polymer brushes and their involvement in the blood–biomaterial contact is discussed. Understanding of the protein interaction with polymeric materials may serve as a basis for development of novel hemocompatible surfaces.

4. Experimental Section/Methods

Materials: CuCl, CuBr, $CuBr_2$, 2,2′-dipyridyl (BiPy), 1,4,8,11-tetramethyl-1,4,8,11-tetraazacyclotetradecane (Me_4Cyclam), phosphate buffered saline (PBS), were purchased from Sigma–Aldrich. ATRP-initiator silane (11-(2-bromo-2-methyl)propionyloxy)undecyltrichlorosilane was synthesized according to the method published earlier).[27] The monomers 3-methacryloylaminopropyl-2-carboxyethyl-dimethylammonium (carboxybetaine methacrylamide, CBMAA), 3-acryloylaminopropyl-2-carboxyethyl-dimethylammonium (carboxybetaine acrylamide, CBAA) and *N*-(2-hydroxypropyl) methacrylamide (HPMA) were synthesized according to literature.[8,18,63,64] The monomers of 2-hydroxyethyl methacrylate (HEMA) and oligo(ethylene glycol) methylether methacrylate Mn=300 Da (MeOEGMA), 2-[(methacryloyloxy)ethyl]dimethyl-3-sulfopropyl ammonium hydroxide (SBMA), and 2- methacryloyloxyethyl phosphorylcholine (PCMA) were purchased from Sigma–Aldrich. Blood and BP was kindly provided by the Institute of Hematology and Blood Transfusion, Prague, Czech Republic. Human blood was collected in tubes containing heparin (1 $U \cdot ml^{-1}$, final concentration). All of the individuals tested agreed to participate in the study on the basis of informed consent. All samples were obtained in

accordance with regulations of the Ethical Committee of the Institute of Hematology and Blood Transfusion, no. EK 3/GA CR/03/2019.

Self-assembled monolayer (SAM) of ATRP initiator: Microscope glass slides and Si wafers were cut into chips of 1cm x 1cm and rinsed with ethanol and DI water twice, dried under flow of nitrogen, and activated in a UV/O_3 cleaner (Jelight) for 20 min. Once activated, they were immediately immersed in a 0.1% v/v solution of ATRP-initiator silane in anhydrous toluene and the container was sealed and placed kept in a dry environment. The silanization reaction was allowed to proceed for 3 h, after which the chips were removed from the solution and rinsed with fresh toluene, acetone, ethanol, and DI water and dried under a stream of nitrogen. The silanized substrates were stored under vacuum.

Polymer brush synthesis: The polymerizations were following our previously published procedures on a substrates coated with a SAM of ATRP-initiator silane.[14] Briefly, a polymerization solution was prepared in inert atmosphere, containing Cu(I) and Cu(II) salts and ligand in degassed solvent. The solution was injected under Ar protection into sealed reactors containing the initiator–SAM-coated substrates and left to react at 30°C for a predefined time to reach the targeted thickness. Subsequently, the reactors were opened and the substrates removed and copiously rinsed with ethanol and water and stored in water. Please consult the corresponding references for a detailed description of the polymerization conditions employed for poly(HEMA),[26] poly(MeOEGMA),[28] poly(SBMA),[27] poly(PCMA), poly(HPMA), poly(CBAA), and poly(HBMA-co-CBMAA).[19]

Physicochemical characterization: The thickness of the polymer brushes was determined by spectroscopic ellipsometry using a J.A. Woollam M-2000X instrument, operating in the wavelength range of λ = 245–1000 nm at an angle of incidence AOI of 60, 65, and 70° in air at room temperature. The thickness and refractive index of polymer layers were obtained from simultaneous fitting of the obtained ellipsometric data using Cauchy relationship model.
The wettability of polymer surfaces was examined by dynamic sessile water drop method using a DataPhysics OCA 20 contact angle system. A 10 µL drop was placed on the surface, and advancing and receding contact angles were determined while the volume of the drop was increased and decreased by 5 µL at flow rate of 0.25 µL·min^{-1}.

X-ray photoelectron spectroscopy (XPS) was measured using a K-Alpha$^+$ instrument (Thermo Scientific, United Kingdom) with a microfocused spot of monochromated Al Kα X-rays and an angle of incidence of 30°. Emitted electrons were collected at a normal angle with respect to the surface and the pass energy for high-resolution XPS spectra was set at 50 eV. Thermo Avantage software was employed for data acquisition and analysis. For quantification, the analyser transmission function, Scofield sensitivity factors, and photoelectron effective attenuation lengths (calculated using the standard TPP-2M formalism) were taken into account. Binding energy scale calibration was performed with the well-known peaks of Cu2p, Ag3d, and Au4f of the respective metals and the C1s peaks of polyethylene terephthalate. High-resolution spectra were fitted with Voigt profiles accounting for the contributions of the individual chemical species. For charge-referencing of the spectra, the binding energy of the C–C, C–H component in the C1s spectrum was set at 285.0 eV.

Mass spectrometry analysis of plasma deposit: Protein digestion was performed directly on the biochip by the addition of 1 ml of 12.5 ng·µl^{-1} trypsin and incubated overnight at 37°C. Digestion was terminated by the addition of formic acid to a final concentration of 2.5%. The obtained peptide mixtures were purified using C18 EmporeTM disks (3M, USA).[65] The peptides were dissolved in 30 µl of 3% acetonitrile/0.1% formic acid. Analyses were performed on a high-capacity ultra-ion-trap mass spectrometer (Bruker Daltonics, Bremen, Germany) with nanoelectrospray ionization coupled to an UltiMate 3000 nanoLC system (Dionex, Sunnyvale, CA, USA) as described in detail previously [66] and on a timsTOF Pro mass spectrometer (Bruker Daltonics, Germany) coupled on-line to an UltiMate 3000 RLSCnano system (Thermo Fisher Scientific, USA). For the timsTOF Pro mass spectrometer, the peptide solution was injected onto an AcclaimTM PepMapTM 100 C18 trapping column (300 µm i.d., 5 mm length, particle size 5 µm, pore size 100 Å; Thermo Fisher Scientific) using an injection volume of 2 µl and a flow rate of 2.5 µl·min^{-1} for 2 min. The peptides were eluted from the trapping column onto an AcclaimTM PepMapTM 100 C18 trapping column (75 µm i.d., 150 mm length, particle size 2 µm, pore size 100 Å; Thermo Fisher Scientific) and separated for 48 min with a linear gradient of 5-35% acetonitrile/0.1% formic acid at a constant rate of 0.3 µl·min^{-1}. The column oven temperature was set at 35°C. MS analysis was operated in PASEF scan mode with positive polarity. Electrospray ionization was performed using a CaptiveSpray (Bruker Daltonics, Germany) with a capillary voltage of 1500 V, dry gas at 3 l·min^{-1}and dry temperature of 180°C. Ions were accumulated for 100 ms, and 10 PASEF MS/MS scans were acquired per topN

acquisition cycle. An ion mobility range (1/K0) was set to 0.6-1.6 $V \cdot s \cdot cm^{-2}$. Mass spectra were collected in the m/z range from 100 to 1700. The polygon filtering was applied to exclude the low m/z singly charged ions. The target intensity was set to 20 000 to repeatedly select precursor for PASEF MS/MS repetitions. Precursors that reached the target intensity were than excluded for 0.4 min. The collision energies were changed from 20 to 59 eV in 5 steps of equal width between 0.6 and 1.6 $V \cdot s \cdot cm^{-2}$ of 1/K0 values.

Raw MS data were processed using MaxQuant software (version 1.6.14) [67] with the integrated Andromeda search engine.[68] The human database downloaded from Uniprot (07. 05. 2021) and the contaminant database included in MaxQant software were used for protein identification. The default parameters for the TIMS-DDA search type and the Bruker TIMS instrument were applied. Trypsin/P was set as an enzyme allowing up to two missed cleavages in a specific digestion mode; carbamidomethylation of cysteine was used as a fixed modification; methionine oxidation and protein N-term acetylation were set as variable modifications; the minimum required peptide length was set to seven amino acids. The precursor ion tolerance was set to 20 and 10 ppm for the first and main peptide searches, respectively; the mass tolerance for MS/MS fragment ions was set to 40 ppm; peptide spectrum match (PSM) and protein identifications were filtered using a target-decoy approach at a false discovery rate (FDR) of 1%. Label-free quantification (LFQ) of proteins was performed using the algorithm integrated into MaxQuant software with the minimum ratio count set to 2.

Hemocompatibility: Seven different surfaces based on polymer brushes of poly(HPMA-co-CBMAA), poly(SBMA), poly(PCMA), poly(MeOEGMA), poly(HEMA), poly(HPMA), poly(CBAA), and control glass surface were incubated with freshly drawn blood from healthy volunteers, and anticoagulated with heparin (1 $U \cdot ml^{-1}$ of heparin, final concentration). The samples (2.5x1.5cm) were incubated in 6 ml of heparinized blood for 1 h under dynamic conditions at 37°C. Subsequently, the blood was directly transferred to the citrate terminating medium and was further processed for ELISA measurement of SC5b-9. The samples with polymer coating and a control glass were thoroughly washed with 0.9% saline and prepared for scanning electron microscopy (SEM). The deposits were fixed by glutaraldehyde (0.5%) for 1 h and subsequently washed with water, ethanol dried, coated with 4 nm thick platinum by sputtering and observed using SEM. Images were evaluated using ImageJ data analysis software. The number of adherent platelets, red blood cells, and leukocytes was determined by

calculating the surface coverage of individual components. Six independent spots were analyzed for each sample. The studies were carried out in triplicate.

Statistical analysis: The fouling data are presented as the mean with the standard deviation (n=3). Statistical differences between individual samples were calculated using Student's T-test. In all cases, the analysis was performed using GraphPad Prism 9.1.1 (GraphPad Software, San Diego, CA, USA), and a p value of $p \leq 0.05$ was considered statistically significant.

Supporting Information

Supporting Information is available from the Wiley Online Library.

Acknowledgements

This work was supported by the Czech Science Foundation (project no. 20-10845S and 21-16729K). A.d.l.S.P acknowledges support from the Czech Academy of Sciences under project MSM200502001. F.D. acknowledges the European Regional Development Fund-Project "Mechanisms and dynamics of macromolecular complexes: from single molecules to cells" (No. CZ.02.1.01/0.0/0.0/15_003/0000441). C.R-E. acknowledge the financial support by the Deutsche Forschungsgemeinschaft (DFG, German Research Foundation) via Schwerpunktprogramm "Towards an Implantable Lung" (Project number: 346972946) and the German Federal Ministry of Education and Research (BMBF) with the project Heart2.0 within the "Bio4MatPro-Competence Center for Biological Transformation of Materials Science and Production Engineering" program (grant no. 031B1154B).

Received: ((will be filled in by the editorial staff))
Revised: ((will be filled in by the editorial staff))
Published online: ((will be filled in by the editorial staff))

References

[1] R. Gbyli, A. Mercaldi, H. Sundaram, K. A. Amoako, *Advanced Materials Interfaces*. **2018**, 5(4), 1700954.
[2] B. D. Ratner, *Journal of biomedical materials research*. **1993**, 27(3), 283-7.
[3] B. D. Ratner, *Biomaterials*. **2007**, 28(34), 5144-7.
[4] I. H. Jaffer, J. I. Weitz, *Acta biomaterialia*. **2019**, 94, 2-10.
[5] G. Makdisi, I. W. Wang, *J Thorac Dis*. **2015**, 7(7), E166-E76.
[6] A. Hucknall, S. Rangarajan, A. Chilkoti, *Advanced Materials*. **2009**, 21(23), 2441-6.

[7] O. Pop-Georgievski, C. Rodriguez-Emmenegger, A. d. l. S. Pereira, V. Proks, E. Brynda, F. Rypáček, *Journal of Materials Chemistry B*. **2013**, 1(22), 2859-67.
[8] C. Rodriguez-Emmenegger, E. Brynda, T. Riedel, M. Houska, V. Šubr, A. B. Alles, E. Hasan, J. E. Gautrot, W. T. S. Huck, *Macromolecular Rapid Communications*. **2011**, 32(13), 952-7.
[9] M. Gorbet, C. Sperling, M. F. Maitz, C. A. Siedlecki, C. Werner, M. V. Sefton, *Acta biomaterialia*. **2019**, 94, 25-32.
[10] D. F. Mosher, *Cardiovascular Pathology*. **1993**, 2(3, Supplement), 149-55.
[11] C. Blaszykowski, S. Sheikh, M. Thompson, *Chemical Society Reviews*. **2012**, 41(17), 5599-612.
[12] Q. Wei, T. Becherer, S. Angioletti-Uberti, J. Dzubiella, C. Wischke, A. T. Neffe, A. Lendlein, M. Ballauff, R. Haag, *Angewandte Chemie (International ed in English)*. **2014**, 53(31), 8004-31.
[13] T. Riedel, Z. Riedelová-Reicheltová, P. Májek, C. Rodriguez-Emmenegger, M. Houska, J. E. Dyr, E. Brynda, *Langmuir*. **2013**, 29(10), 3388-97.
[14] C. Rodriguez Emmenegger, E. Brynda, T. Riedel, Z. Sedlakova, M. Houska, A. B. Alles, *Langmuir*. **2009**, 25(11), 6328-33.
[15] S. M. Slack, Y. Cui, V. T. Turitto, *Thromb Haemost*. **1993**, 70(07), 129-34.
[16] M. Krishnamoorthy, S. Hakobyan, M. Ramstedt, J. E. Gautrot, *Chemical Reviews*. **2014**, 114(21), 10976-1026.
[17] M. Forinová, A. Pilipenco, I. Víšová, N. S. Lynn, J. Dostálek, H. Mašková, V. Hönig, M. Palus, M. Selinger, P. Kočová, F. Dyčka, J. Štěrba, M. Houska, M. Vrabcová, P. Horák, J. Anthi, C.-P. Tung, C.-M. Yu, C.-Y. Chen, Y.-C. Huang, P.-H. Tsai, S.-Y. Lin, H.-J. Hsu, A.-S. Yang, A. Dejneka, H. Vaisocherová-Lísalová, *ACS Applied Materials & Interfaces*. **2021**, 13(50), 60612-24.
[18] H. Vaisocherová, W. Yang, Z. Zhang, Z. Cao, G. Cheng, M. Piliarik, J. Homola, S. Jiang, *Analytical Chemistry*. **2008**, 80(20), 7894-901.
[19] T. Riedel, F. Surman, S. Hageneder, O. Pop-Georgievski, C. Noehammer, M. Hofner, E. Brynda, C. Rodriguez-Emmenegger, J. Dostálek, *Biosensors & bioelectronics*. **2016**, 85, 272-9.
[20] L. Witzdam, Y. L. Meurer, M. Garay-Sarmiento, M. Vorobii, D. Söder, J. Quandt, T. Haraszti, C. Rodriguez-Emmenegger, *Macromolecular Bioscience*. **2022**, 22(5), 2200025.
[21] M. Garay-Sarmiento, L. Witzdam, M. Vorobii, C. Simons, N. Herrmann, A. de los Santos Pereira, E. Heine, I. El-Awaad, R. Lütticken, F. Jakob, U. Schwaneberg, C. Rodriguez-Emmenegger, *Advanced Functional Materials*. **2022**, 32(9), 2106656.
[22] S. Dedisch, F. Obstals, A. de los Santos Pereira, M. Bruns, F. Jakob, U. Schwaneberg, C. Rodriguez-Emmenegger, *Advanced Materials Interfaces*. **2019**, 6(18), 1900847.
[23] F. Obstals, L. Witzdam, M. Garay-Sarmiento, N. Y. Kostina, J. Quandt, R. Rossaint, S. Singh, O. Grottke, C. Rodriguez-Emmenegger, *ACS Appl Mater Interfaces*. **2021**, 13(10), 11696-707.
[24] K. A. Woodhouse, J. I. Weitz, J. L. Brash, *Biomaterials*. **1996**, 17(1), 75-7.
[25] J. L. Brash, *Journal of Biomaterials Science, Polymer Edition*. **2000**, 11(11), 1135-46.
[26] T. Riedel, A. de los Santos Pereira, J. Táborská, Z. Riedelová, O. Pop-Georgievski, P. Májek, K. Pečánková, C. Rodriguez-Emmenegger, *Macromolecular Bioscience*. **2022**, 22(3), 2100460.
[27] C. Rodriguez-Emmenegger, S. Janel, A. de los Santos Pereira, M. Bruns, F. Lafont, *Polymer Chemistry*. **2015**, 6(31), 5740-51.
[28] A. de los Santos Pereira, T. Riedel, E. Brynda, C. Rodriguez-Emmenegger, *Sensors and Actuators B: Chemical*. **2014**, 202, 1313-21.

[29] T. Riedel, S. Hageneder, F. Surman, O. Pop-Georgievski, C. Noehammer, M. Hofner, E. Brynda, C. Rodriguez-Emmenegger, J. Dostálek, *Analytical Chemistry*. **2017**, 89(5), 2972-7.
[30] X. Li, S. Silge, A. Saal, G. Kircher, K. Koynov, R. Berger, H.-J. Butt, *Langmuir*. **2021**, 37(4), 1571-7.
[31] S. Desseaux, J. P. Hinestrosa, N. Schüwer, B. S. Lokitz, J. F. Ankner, S. M. Kilbey, K. Voitchovsky, H.-A. Klok, *Macromolecules*. **2016**, 49(12), 4609-18.
[32] Z. Yang, S. Zhang, V. V. Tarabara, M. L. Bruening, *Macromolecules*. **2018**, 51(3), 1161-71.
[33] A. Kostruba, Y. Stetsyshyn, S. Mayevska, M. Yakovlev, P. Vankevych, Y. Nastishin, V. Kravets, *Soft Matter*. **2018**, 14(6), 1016-25.
[34] Z. Zhang, J. A. Finlay, L. Wang, Y. Gao, J. A. Callow, M. E. Callow, S. Jiang, *Langmuir*. **2009**, 25(23), 13516-21.
[35] J. N. Barbosa, M. C. L. Martins, S. C. Freitas, I. C. Gonçalves, A. P. Águas, M. A. Barbosa, *Journal of Biomedical Materials Research Part A*. **2010**, 93A(1), 12-9.
[36] S. A. Smith, R. J. Travers, J. H. Morrissey, *Crit Rev Biochem Mol Biol*. **2015**, 50(4), 326-36.
[37] Y. Wu, *Thromb J*. **2015**, 13, 17-.
[38] Y. Mödinger, G. Q. Teixeira, C. Neidlinger-Wilke, A. Ignatius, *Int J Mol Sci*. **2018**, 19(11).
[39] J. M. Anderson, A. Rodriguez, D. T. Chang, *Semin Immunol*. **2008**, 20(2), 86-100.
[40] J. R. Dunkelberger, W. C. Song, *Cell Res*. **2010**, 20(1), 34-50.
[41] A. d. l. S. Pereira, C. Rodriguez-Emmenegger, F. Surman, T. Riedel, A. B. Alles, E. Brynda, *RSC Advances*. **2014**, 4(5), 2318-21.
[42] R. A. Latour, *Colloids Surf B Biointerfaces*. **2020**, 191, 110992-.
[43] B. Sivaraman, R. A. Latour, *Biomaterials*. **2010**, 31(5), 832-9.
[44] F. Surman, T. Riedel, M. Bruns, N. Y. Kostina, Z. Sedláková, C. Rodriguez-Emmenegger, *Macromolecular Bioscience*. **2015**, 15(5), 636-46.
[45] J. B. Schlenoff, *Langmuir*. **2014**, 30(32), 9625-36.
[46] L. Digiacomo, F. Cardarelli, D. Pozzi, S. Palchetti, M. A. Digman, E. Gratton, A. L. Capriotti, M. Mahmoudi, G. Caracciolo, *Nanoscale*. **2017**, 9(44), 17254-62.
[47] R. M. Cornelius, J. Macri, K. M. Cornelius, J. L. Brash, *Langmuir*. **2015**, 31(44), 12087-95.
[48] R. M. Cornelius, J. Macri, K. M. Cornelius, J. L. Brash, *Biointerphases*. **2016**, 11(2), 029810.
[49] R. M. Cornelius, J. Macri, J. L. Brash, *Journal of Biomedical Materials Research Part A*. **2011**, 99A(1), 109-15.
[50] F. A. Orsi, W. M. Lijfering, A. Van der Laarse, L. R. Ruhaak, F. R. Rosendaal, S. C. Cannegieter, C. Cobbaert, *Clinical epidemiology*. **2019**, 11, 625-33.
[51] M. van der Stoep, S. J. A. Korporaal, M. Van Eck, *Cardiovascular Research*. **2014**, 103(3), 362-71.
[52] L. M. Vogt, E. Kwasniewicz, S. Talens, C. Scavenius, E. Bielecka, K. N. Ekdahl, J. J. Enghild, M. Mörgelin, T. Saxne, J. Potempa, A. M. Blom, *The Journal of Immunology*. **2020**, 204(10), 2779-90.
[53] G. Gunkel, W. T. S. Huck, *Journal of the American Chemical Society*. **2013**, 135(18), 7047-52.
[54] G. A. Manderson, M. Martin, P. Önnerfjord, T. Saxne, A. Schmidtchen, T. E. Mollnes, D. Heinegård, A. M. Blom, *Molecular Immunology*. **2009**, 46(16), 3388-98.

[55] A. L. Jones, M. D. Hulett, C. R. Parish, *Immunology & Cell Biology*. **2005**, 83(2), 106-18.
[56] J. L. MacQuarrie, A. R. Stafford, J. W. Yau, B. A. Leslie, T. T. Vu, J. C. Fredenburgh, J. I. Weitz, *Blood*. **2011**, 117(15), 4134-41.
[57] T. K. Truong, R. A. Malik, X. Yao, J. C. Fredenburgh, A. R. Stafford, H. M. Madarati, C. A. Kretz, J. I. Weitz, *Journal of Thrombosis and Haemostasis*. **2022**, 20(4), 821-32.
[58] A. Aliyandi, C. Reker-Smit, R. Bron, I. S. Zuhorn, A. Salvati, *ACS Biomaterials Science & Engineering*. **2021**, 7(12), 5573-84.
[59] K. T. Preissner, *Annual review of cell biology*. **1991**, 7, 275-310.
[60] X. Gao, Z. Xu, *Acta Biochimica et Biophysica Sinica*. **2008**, 40(7), 619-24.
[61] P. Gunnarsson, L. Levander, P. Påhlsson, M. Grenegård, *The FASEB Journal*. **2007**, 21(14), 4059-69.
[62] H. C. Cohen, D. C. Frost, T. J. Lieberthal, L. Li, W. J. Kao, *Biomaterials*. **2015**, 50, 47-55.
[63] C. Rodriguez-Emmenegger, M. Houska, A. B. Alles, E. Brynda, *Macromol Biosci*. **2012**, 12(10), 1413-22.
[64] K. Ulbrich, V. Subr, J. Strohalm, D. Plocová, M. Jelínková, B. Ríhová, *Journal of controlled release : official journal of the Controlled Release Society*. **2000**, 64(1-3), 63-79.
[65] J. Rappsilber, M. Mann, Y. Ishihama, *Nature Protocols*. **2007**, 2(8), 1896-906.
[66] K. Pecankova, P. Pecherkova, Z. Gasova, Z. Sovova, T. Riedel, E. Jäger, J. Cermak, P. Majek, *PLOS ONE*. **2022**, 17(1), e0262484.
[67] J. Cox, M. Mann, *Nature Biotechnology*. **2008**, 26(12), 1367-72.
[68] J. Cox, N. Neuhauser, A. Michalski, R. A. Scheltema, J. V. Olsen, M. Mann, *Journal of Proteome Research*. **2011**, 10(4), 1794-805.